SEDIMENT TRANSPORT IN THE WESTERN INTERIOR SEAWAY OF NORTH AMERICA: PREDICTIONS FROM A CLIMATE-OCEAN-SEDIMENT MODEL

RUDY SLINGERLAND
Department of Geosciences, The Pennsylvania State University, University Park, Pennsylvania 16802 U.S.A.
AND
TIMOTHY R. KEEN
Naval Research Laboratory, Oceanography Division, Stennis Space Center, Mississippi 39529 U.S.A.

ABSTRACT: Whether from the foreshore, shoreface, shelf, or incised estuarine valleys, sedimentary deposits along the western edge of the Western Interior seaway quite uniformly record southerly directed paleoflows. Cardium Formation shoreface gravels at Willesden Green, Alberta, decrease in clast size to the southeast. Isoliths outlining clastic wedges, such as the Chalk Creek, are recurved to the south. Large-scale cross-strata in rocks considered to be either shelf sand ridges or detached shorefaces, such as the Kakwa and Musreau Members of the Cardium Formation and the Straight Cliffs Formation of southwestern Utah, indicate southerly directed paleocurrents. Estuarine incised valley-fills trend south or southeast, reflecting a high-stand shelf topography inherited by rivers as they cut across the inner shelf in response to a high-order sea-level drop. To explain this uniformity we conducted two numerical experiments that predict circulation and sediment transport paths in the seaway in response to 1) mean annual atmospheric forcing and 2) the passage of a mid-latitude winter storm. The mean annual forcing for the early Turonian is computed by GENESIS, an NCAR global climate model; the cyclone is computed using an idealized hurricane model. For the mean annual experiment, circulation of the seaway is computed using a three-dimensional, turbulent flow, coastal ocean model under the following initial and boundary conditions: 1) paleobathymetry according to a new interpretation of the litho- and bio-stratigraphy for the early Turonian; 2) fresh water runoff and precipitation-evaporation magnitudes as computed by GENESIS; 3) temperatures and salinities of the Boreal and Tethys Oceans based on GENESIS atmospheric temperatures; and 4) mean annual and daily wind stresses computed by GENESIS. For the storm experiment, circulation is forced solely by wind stresses.

Results show that these boundary conditions combine to produce a basin-wide counterclockwise gyre that arises from Coriolis acceleration acting on runoff jets trapped along the coast, abetted by latitudinal temperature and salinity gradients and a north-south, wind shear-couple. Individual storm events reverse the general circulation locally, but summed over a storm's duration, the storm-driven fluid and sediment transport augments the mean-annual transport of the gyre. Thus, net sediment transport directions along the western margin of the seaway, both on the shelf and in the wave-driven littoral zone, were southerly because the mean annual wind field, latitudinal temperature gradient, and fresh water runoff from land created a background circulation consisting of southerly geostrophic flow there. In addition, counterclockwise rotating, mid-latitude cyclonic storms passing southeastward over the central seaway drove a net southerly littoral drift in the foreshore and shore-parallel geostrophic flows whose net sediment transport was southerly. Along the eastern margin the computed shelf and littoral transport was to the north.

INTRODUCTION

The origin of isolated shallow-marine sandbodies is unknown, and nowhere is answering this question more vexing than along the western margin of the Cretaceous interior seaway. Examples there include the Shannon Sandstone (Spearing, 1976; Seeling, 1978; Shurr, 1984; Swift and Rice, 1984; Gaynor and Swift, 1988; Tillman and Martinsen, 1984, 1987; Walker and Bergman, 1993; Bergman, 1994), Eagle Sandstone (Rice, 1976, 1980; Rice and Shurr, 1983; this volume), Tocito Sandstone, (Snedden and Nummedal, 1990; Nummedal and Riley, 1991; Valasek, 1995; Jennette and Jones, 1995), and Viking Formation (Evans, 1970; Hein et al.,1986; Leckie, 1986; Raddysh, 1988; Power, 1988; Downing and Walker, 1988; Posamentier and Chamberlain, 1993; Walker, 1995; Walker and Wiseman, 1995), all of which have been variously interpreted as offshore sand ridges, incised estuarine valley fills, or incised shoreface deposits. In each case, sedimentological paleoflow indicators, such as the type, scale, and orientation of bedforms and sediment textures, have played an important role in the interpretation. Whether these sedimentological indicators can be used to differentiate among the different interpretations depends on what bedforms, textures, and transport directions we expect along the western margin of the seaway in these various depositional settings. These expectations are usually derived from modern analogs (e.g., Part 2, this volume), but this is always risky because argument by analogy only succeeds if all other factors forcing circulation in the modern and ancient basins, such as the regional climate, are similar.

The purpose of this paper is to provide an alternative basis for interpreting paleoflow indicators and sedimentary textures observed in coastal and shelf sediments of the Western Interior seaway. Here we deduce the expected circulation and sediment transport paths in the seaway from first principles using a climate/ocean/sedimentation model. Admittedly, this method too has its pitfalls. While based on the conservation laws, climate/ocean/sedimentation models parameterize some important processes and by computational necessity must be run at coarse resolution. More importantly, the accuracy of the results is strongly dependent upon the initial conditions and the boundary conditions. Nevertheless, given our present best estimates of the seaway's paleogeography, paleobathymetry, and paleoclimate, these computations should provide the best estimate to date of the seaway's circulation and sediment transport because they constrain the complex sedimentary processes using fundamental principles of mass, energy, and momentum conservation.

Early conjectures on the circulation of the seaway relied upon intuition and analogy with modern oceans (see Parrish, Gaynor, and Swift, 1984; or Hay, Eicher, and Diner, 1993). Attempts to compute the circulation of the seaway from first principles started with Parrish et al. (1984), who computed the wind-driven circulation in present-day Colorado and Wyoming. Slater (1985) calculated the independent tides of the seaway using a primitive equation model and concluded that the tides were microtidal everywhere. Subsequent calcu-

Isolated Shallow Marine Sand Bodies: Sequence Stratigraphic Analysis and Sedimentologic Interpretation.
SEPM Special Publication No. 64, Copyright © 1999
SEPM (Society for Sedimentary Geology), ISBN 1-56576-057-3, p. 179-190.

lations of the co-oscillating tides by Ericksen and Slingerland (1990) suggested that they were larger but still microtidal, with the exception of the southeastern coast. Ericksen and Slingerland also computed the wind-driven circulation of the entire seaway in response to mean annual winds and a mid-latitude extratropical storm. More recent circulation hindcasts (Slingerland et al., 1996; Jewell, 1996) have included thermohaline forcing as well as mean annual winds. None of these studies has attempted to compute sediment transport in the seaway.

Here we present results from the first climate/ocean/sedimentation computations for the seaway. They show that the net sediment transport direction along the western margin of the seaway in offshore sand ridges, incised estuarine valley fills, and incised shoreface deposits should have been to the south. These predictions are consistent with paleoflow observations there, which indicate a spatially and temporally uniform net sediment transport to the south.

METHODOLOGY

To calculate the sediment transport rates and directions in the Western Interior seaway, one must compute the expected atmospheric forcing and resulting wind-driven and thermohaline flows, as well as oscillatory currents associated with surface waves. The steady and oscillatory currents must then be combined using an appropriate bottom boundary layer model (BBLM) to compute bottom shear stresses. Given the history of bed stresses, sediment transport rates and directions must then be calculated using a sediment transport and bed conservation model. Two cases are presented: Case I) sediment transport due to mean annual thermohaline and wind-driven circulation, and Case II) sediment transport during an 8-day storm.

Sediment Transport Due to Thermohaline and Wind-driven Circulation

Atmospheric forcing for this case comes from the climate for the early Turonian as computed by GENESIS, a global climate model developed by Pollard and Thompson (1992) at the National Center for Atmospheric Research and reported in earlier studies by Barron, Fawcett, Pollard, and Thompson (1993) and Slingerland et al. (1996). GENESIS consists of an atmospheric general circulation model (AGCM) coupled to surface models of soil, snow, sea-ice and a slab ocean, and includes a Land-Surface-Transfer Model that computes near-surface fluxes of heat, moisture, and momentum in the presence of vegetation. The AGCM is an extensively modified version of the National Center for Atmospheric Research Community Climate Model version 1 (CCM1). Each of the seasonal cycle experiments is executed for 12 years to bring the model into dynamic equilibrium; values of atmospheric variables for the subsequent three years are stored for later analysis. These experiments are based on the continental paleogeography and topography of Barron (1987) with atmospheric CO_2 concentrations four times the present day value.

The wind-driven and thermohaline circulation of the seaway for the mean annual case is taken from Slingerland et al. (1996), who calculated it using CIRC, a coastal ocean model derived by Leendertse (Leendertse and Liu, 1977; Keen and Slingerland, 1993). Shoreline positions and depth contours were based on the relationships between lithofacies and depths observed in modern marine settings, and supported by biofacies data from selected sites within the basin (see Slingerland et al., 1996, for a discussion). Precipitation or evaporation over the seaway in that study was simulated by adding or subtracting fresh water from the upper layer of the seaway in proportion to the net precipitation hindcast by GENESIS. Fresh-water runoff from the adjacent continent entered the model seaway through 18 rivers spaced roughly every 4° latitude along the seaway's eastern and western shorelines. River discharges into the seaway were set equal to the precipitation minus evaporation for each river's drainage basin. Surface shear stresses arising from the mean annual wind field were applied to each wet node in CIRC. Output of the model consisted of U, V, and W velocities, temperature, salinity, and water surface elevations. After 7 years of spin-up, the model system approached dynamic equilibrium. At that point the mass of water entering the seaway through precipitation, runoff, and counterflow at the entrances was balanced by the mass leaving by evaporation and surface flows to the world ocean.

Because the resulting circulation is relatively weak, we do not compute the surface wave field, bottom bed stresses, and bed conservation for this case. Instead we qualitatively discuss the implications for fine-grained sediment transport.

Sediment Transport During an 8-Day Storm

The experiment that simulated sediment transport during the passage of a storm over the seaway was forced by an ideal, extratropical winter cyclone. We defined an average storm track across the seaway using the standard deviation of the geopotential height field as computed by GENESIS (Ericksen and Slingerland, 1990). Along the track we passed an ideal cyclone using the cyclone model discussed in Keen and Slingerland (1993). The forward storm speed is 10 m/s, the pressure difference is 53 mm of mercury, and the maximum radius is 1000 km. The simulation starts at day zero when the storm center is northwest of the seaway and ends 8 days later after it has passed to the southeast.

The resulting wind-driven circulation in the seaway was computed using the Princeton Ocean Model (POM) (Blumberg and Mellor, 1987; Mellor, 1993; for its previous application to the Western Interior seaway, see Jewell, 1996). POM is a primitive equation ocean model that uses a free surface and sigma coordinate system. Vertical mixing is computed using the turbulence closure sub-model of Mellor and Yamada (1982). The model grid consists of 112 x 260 nodes in the horizontal, spaced 30 km apart, and 11 sigma coordinates; model external time-step is 100 seconds. POM is initialized from an experiment in which the circulation was driven solely by mean annual winds as computed by GENESIS. The northern and southern open boundaries of the basin are treated using a radiation boundary condition with water surface elevations relaxed to interior values.

The bathymetry and boundary geography for Case II are given in Figure 1. Minimum water depth is 10 m; maximum is 950 m. Sediment in the seaway consists of two types. In water depths shallower than 30 m the bed consists of five size classes of very fine sand with a mean grain size of 2.5 ϕ and a standard deviation equal to 1 ϕ. In waters deeper than 30 m the bed consists of 5 size classes with a mean size of 7.5 ϕ and a standard deviation of 2 ϕ.

Storm waves are computed from the wind field using the forecasting equations for fetch-limited conditions (Corps of Engineers, 1984):

$$H_s = 5.112x10^{-4} U_a \sqrt{f} \qquad \text{(EQ 1)}$$

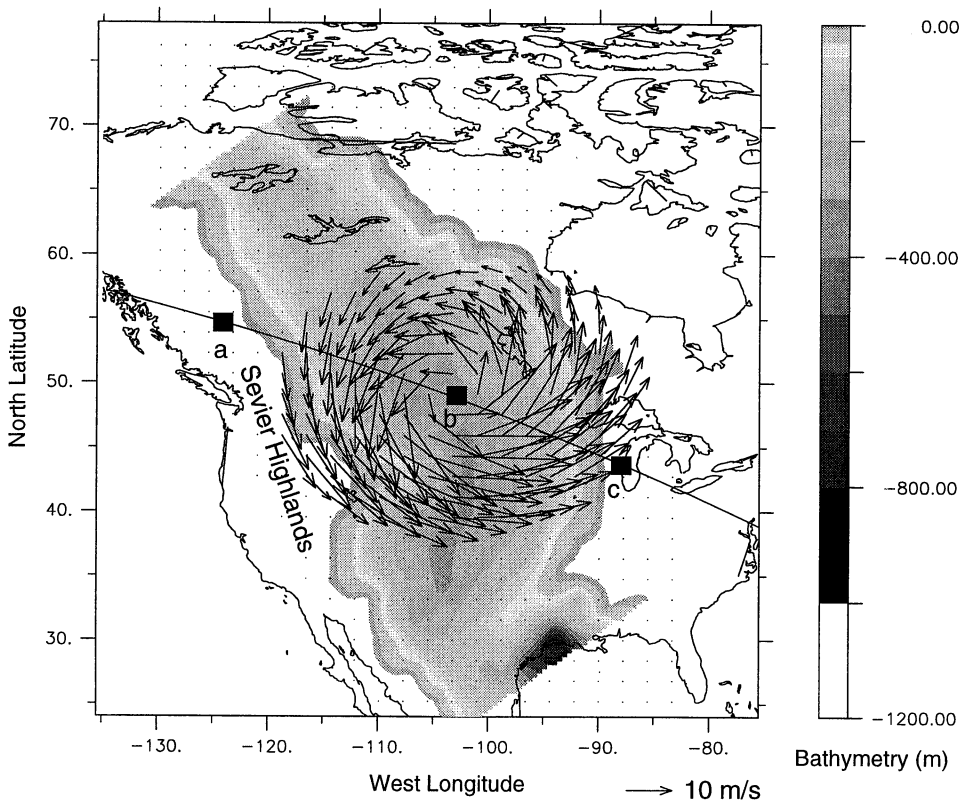

Fig. 1.—Paleobathymetric map of the Early Turonian *W. coloradoense* Biozone in the western interior basin (redrawn from Sageman and Arthur, 1994). In one numerical experiment an idealized extra-tropical cyclone passes from west to east along the solid line. Solid squares represent location of storm eye at a) 2.17, b) 4.14, and c) 6.13 days after the start of computations. Wind speed magnitudes indicated by arrow at bottom right.

$$T_m = 6.238x10^{-2}\sqrt[3]{U_a f} \qquad \text{(EQ 2)}$$

where H_s = significant wave height (m); U_a = adjusted wind speed (m/s), given by:

$$U_a = 0.71U^{1.23} \qquad \text{(EQ 3)}$$

where U = wind speed (m/s) at 10 m above the water surface, f = fetch (m), and T_m = period (s) of the peak of the wave spectrum. The wave propagation direction is set equal to the wind direction. Wave height and period are then used to compute the wave orbital amplitude and speed in the wave bottom boundary layer using linear wave theory.

Suspended sediment profiles are computed using the Glenn and Grant (1987) suspended-sediment, stratified BBLM with modifications discussed by Keen and Glenn (1994). The unidirectional current driving the BBLM is taken from POM's lowest layer. The bottom roughness is computed by the BBLM and is dependent on sediment characteristics as well as the combined wave-current flow. An active layer is defined as the height of ripples plus the thickness of the near-bed sediment transport layer (Grant and Madsen, 1982). This layer represents interactions between the bed and the flow during a model time step. Sediment resuspension and erosion cannot exceed the active layer depth, thereby greatly reducing the erosion of fine material reported previously (e.g., Keen and Slingerland, 1993). Suspended sediment transport rates are computed from the sediment and current profiles computed by the BBLM at each point. A bed conservation equation is solved at each model grid point to calculate regions of erosion or deposition for each sediment size.

RESULTS

Case I: Mean Annual Circulation and Sediment Transport

As reported in Slingerland et al. (1996), the steady-state surface circulation of the seaway (Fig. 2) consists of a basin-scale counterclockwise gyre. This flow extends to the bed in all water depths less than about 100 m. On the eastern shelf currents flow to the north; on the western shelf currents flow to the south. Surface currents are on the order of a few centimeters per second. Below 100 m, waters collect in the core of the seaway through weak caballing and flow along its thalweg, exiting to the north and south.

This simple estuarine circulation owes its existence to a relatively complex forcing. Sensitivity studies in which the circulation was computed independently for each forcing factor indicate that the density and wind-driven flows are additive, with the thermohaline forcing being the strongest. Fresh and therefore buoyant river water enters the seaway from its eastern and western margins and creates offshore-dipping water-surface slopes, down which this buoyant water subsequently flows. In the process it is deflected to the right by the Coriolis force and piles up along each coast, until the offshore pressure force arising from the surface slope just balances the Coriolis force. This water then moves along

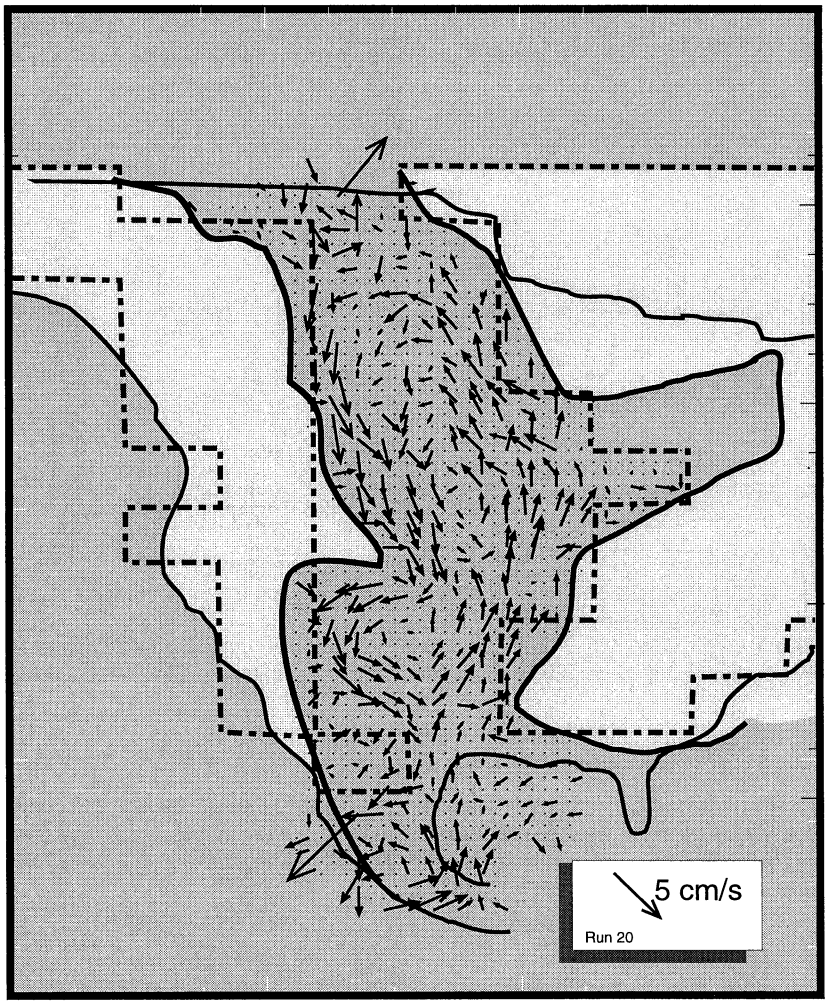

Fig. 2.—Mean annual steady-state circulation in top 10 meters of water column as hindcast by a coastal ocean model subject to atmospheric forcing computed by a global climate model (from Slingerland et al., 1996). Dash line represents paleogeography of North America seen by GENESIS. Circulation in the seaway consists of a large cyclonic gyre.

isobaths as geostrophically confined jets, avoiding the center of the seaway.

The shear couple arising from the coastal jets, and water surface slopes arising from contraction of the water column as it densifies toward the basin center, draw Boreal and Tethyan surface waters into the seaway where they mix as they shear past one another. The mixed waters, being denser than either component, downwell, split into two flows, and return to the global ocean, with 60% of the flux into the Boreal Ocean.

No sediment transport was computed for the mean annual circulation in Slingerland et al. (1996). We can conjecture however, that during fair weather this background circulation would advect suspended sediment delivered to the shelf by river plumes, much as muds of the Amazon are carried north along the Guiana coast by the Guiana Current. Consequently, fair weather, fine-grained sediment transport in the seaway should follow the trajectories shown in Figure 2.

This isn't the whole story of course, because sediment transport rates are proportional to a high power of flow velocity. Consequently, the bulk of sediment transport on the shelf, shoreface, and in the nearshore of the seaway must have occurred during storms, much as occurs on today's continental shelves (Swift et al., 1979; Madsen et al., 1993; Vincent, Young, Swift, 1983; Wright, Xu, and Madsen, 1994; Green et al., 1995).

Case II: Storm-driven Circulation and Sediment Transport

Superimposed on the mean annual circulation of the seaway must have been the stronger but shorter duration flows caused by storms. If modern shelves are the key to the past, then these flows consisted of two parts, an oscillatory component due to water surface waves and a wind and pressure gradient-driven, quasi-steady component. As discussed above, the time integral of these two components determines the net sediment transport magnitude and direction.

Here the time integral is computed during a model storm's transit across the seaway. Initially, the storm eye is located over the Sevier Highlands (Fig. 1) and weaker winds at the front of the storm blow predominantly to the north, parallel to shore. By day 2 (Fig. 1, location a), winds blow

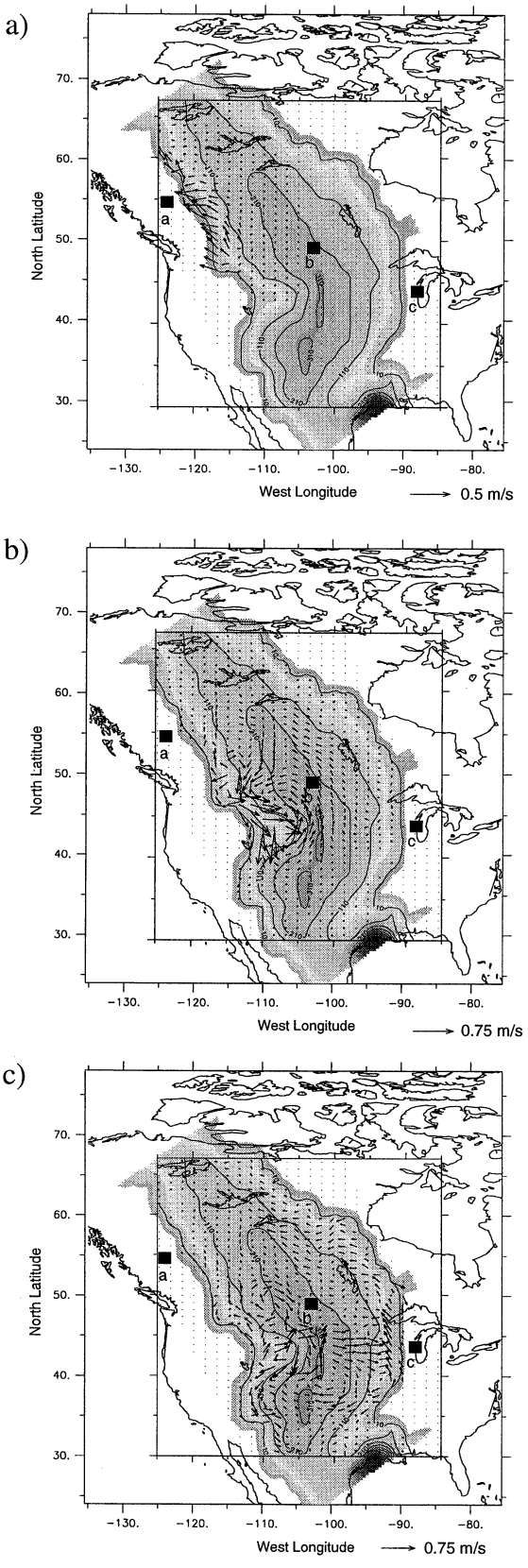

predominantly offshore along the U.S. portion of the seaway and onshore in northern Alberta. Bottom currents computed by POM at this time are northerly and onshore (Fig. 3a) along the Canadian portion of the seaway's west coast. This pattern arises because of geostrophy and because the water motion reflects the history of wind stresses. As the wind stress accelerates surface waters downwind (northward), a cross-stream Coriolis force is created that deflects the surface waters to the right (offshore). Sea levels fall along the coast until a cross-shelf water surface slope creates a shoreward-directed pressure force of sufficient magnitude to balance the Coriolis force. Bottom waters, being loosely decoupled from the wind stress, sense the water surface slope and flow down it. Thus, their net motion is northward and shoreward.

The wind sea (shown for day 4 in Fig. 4) consists of asymmetric distributions of wave heights and periods that decrease away from the storm center. Higher values occur to the south due to the higher winds there (c.f., Fig. 1 and Fig. 2). This pattern is translated self-similarly as the storm eye advances, and therefore the wind sea on day 2 can be reconstructed by recentering the distributions shown in Figure 4 on site a. The direction of wave advance is assumed to be coparallel with the local wind vectors.

As noted above, early in the storm's transit, winds blow predominantly alongshore to the north. The wind sea then should consist of waves between zero and 6 m high with periods of less than 9 s approaching the coast from the south. These waves should create a littoral drift to the north. South of the storm track strong winds blow offshore, creating a wave field that propagates offshore at a right angle to the wind-driven currents.

The nonlinear interaction between the quasi-steady and oscillatory currents in the bottom boundary layer creates the bed stress that entrains and transports sediment. The magnitude of the bed stress as computed in the BBLM is not only a function of the magnitudes of the waves and currents but also of water depth—because bottom wave orbital parameters vary with location in the water column—and sediment type—because turbulence damping due to suspended sediment and friction due to bedforms varies with grain size. Regions of significant bed stress on day 2 (Fig. 5a) are restricted to two regions shallower than 30 m: a region spanning about 10° latitude immediately south of the storm track and a much smaller region to the north. These are regions of both significant waves and wind-driven currents. Sediment in transport moves northward and shoreward at this time (Fig. 3).

By day 4, the storm has progressed to the center of the seaway (Fig. 1) such that winds are predominantly north-directed on the east coast and south-directed on the west coast. In response to this evolving wind field, the storm currents are significantly intensified and reoriented (Fig. 3b). A vast region of the western shelf from the U.S.-Canadian border to southern Colorado is swept by currents that average 0.5 m/s. In waters shallower than about 100 m, the currents are roughly coast parallel and southerly with a small offshore component. North

←

Fig. 3.—Bottom currents as computed by POM at 5 m above the bed after: a) 2.17 days of simulation when the strongest winds are restricted to the western margin of the basin; b) 4.14 days when the storm is in the center of the basin; and c) 6.13 days as the storm approaches the eastern margin.

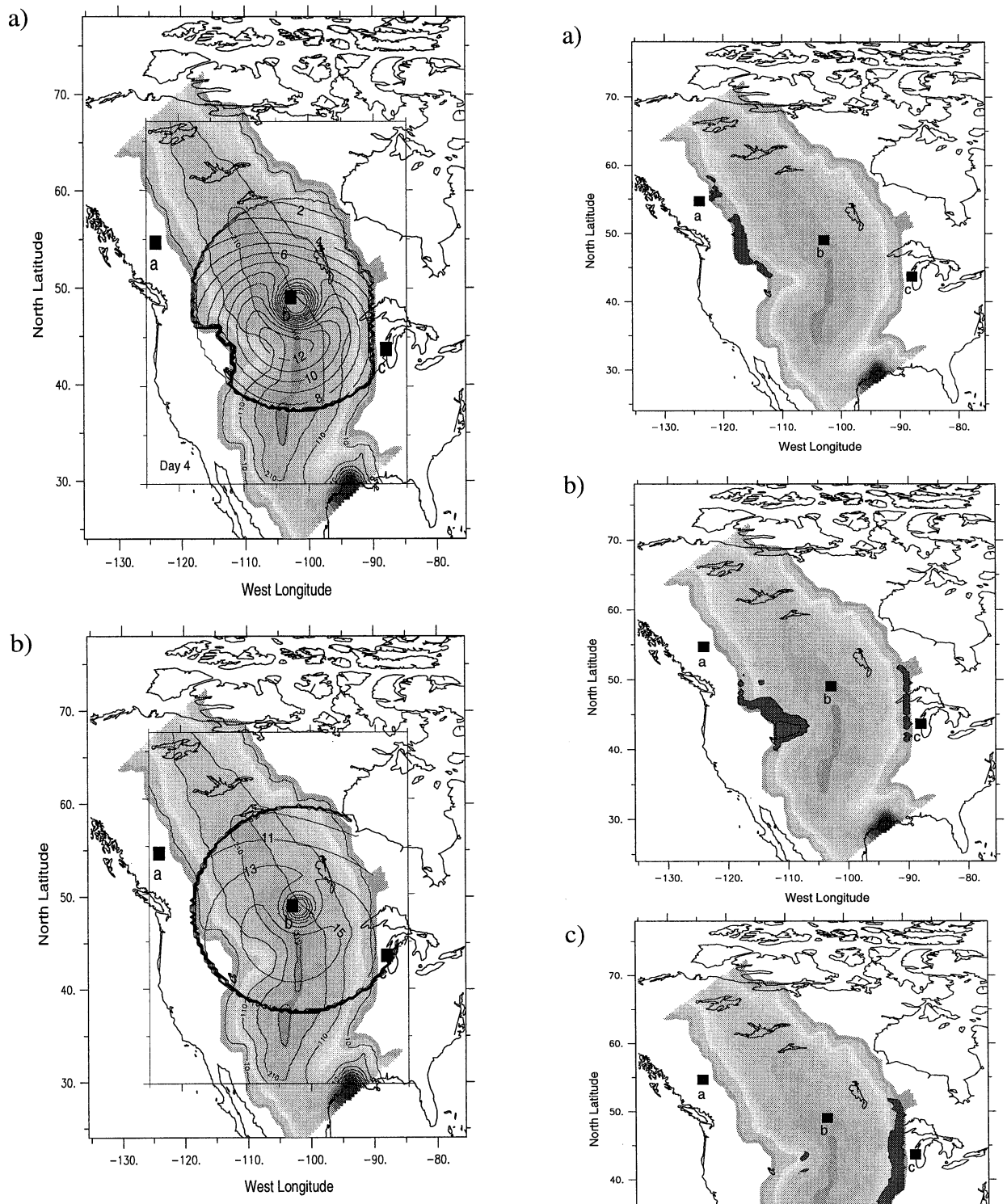

Fig. 4.—Wind sea at day 4.14. a) Significant wave heights (m) as computed by Equation 1 (1 m contour interval). Values range from 0 to 12 m, with highest wave heights occurring on south side of storm where winds speeds are highest. Wave direction and consequently orientation of oscillatory stroke are assumed to follow local wind vectors (Fig. 1); b) Significant wave periods (seconds) computed by Equation 2 (2 second contour interval).

of the border the shelf currents diminish and turn north. Currents on the east coast are still weak. The currents flow onshore in the north and offshore in the south in deeper waters. These bottom currents are isobathyal geostrophic currents, similar to currents on the east coast of the United States during a nor'easter (Lee et al., 1985).

Along the western shelf in the region of strong bottom flow, the wind sea (Fig. 4) increases in height and period from 5 m and 11 second waves in the north to a maximum of 12 m, 15 second waves in the south. As expected, this combination of currents and waves leads to a region of high bed-shear stress (Fig. 5b) centered on the Montana-Wyoming promontory. Along the east coast an extensive region of shallow water experiences modest shear stresses, mainly due to the wind sea.

By day 6 the storm eye has passed over the eastern coast (Fig. 1). Consequently winds blow predominantly to the south along the eastern shelf. Bottom currents (Fig. 3c) now comprise a melange of forced and relaxation flows. Bottom currents along the western shelf are primarily driven by a barotropic Kelvin wave propagating counterclockwise along the western shelf. Bottom currents along the eastern shelf are a result of downwelling associated with coastal setup and relaxation flows as the wind stress decreases. The wind sea is now confined to the eastern shelf. Although wind-driven flows are still relatively strong on the western shelf, significant bottom shear stresses (Fig. 5c) are principally confined to shallow waters of the eastern shelf, reflecting the importance of the storm waves there.

The net sediment transport arising from this complicated history of bed-shear stress magnitudes and directions is given in Figure 6. In this plot, the direction of sediment transport has been taken into account in integrating the sediment flux so that if sediment at a site first moves north and then south at the same rate and for the same duration, then the net transport rate at the site will be zero. The net sediment transport direction on the western shelf is roughly isobathyal to the south. Highest magnitudes occur on the Montana-Wyoming promontory, where sediment is transported in water depths of up to 100 m. On the eastern shelf, net transport is to the north with lower magnitudes. The small magnitude arises partly because southerly transport during the latter stages of the storm's passage cancel northerly transport earlier in the storm's transit.

The bulk of the material transported is sand from the inner shelf, where the greatest shear stresses are calculated. Limited transport occurs offshore because the shear stresses are weaker there and the active layer is quite thin.

Two storm beds remain after the storm passes, one on the western shelf and one on the eastern shelf (Fig. 7). Both span about 15° of latitude and are confined to waters shallower than 100 m. Thickness ranges from a seaward feather-edge to 54 cm in about 20 m of water. The bed consists predominantly of very fine sand.

In summary, although the quasi-steady and oscillatory currents arising from the passage of an extratropical storm are multidirectional, the computed net sediment transport on the western margin of the seaway is southerly, reinforcing finer-grained sediment transport to the south due to the mean annual circulation. Consequently, we also expect the observed paleoflow indicators and sedimentary textures from foreshore, shoreface, and offshore settings in the region of the Cretaceous storm track to record this southward transport.

EVIDENCE FOR SOUTHERLY SEDIMENT TRANSPORT

Evidence for southerly sediment transport along the western margin of the Cretaceous Interior seaway has been obtained by numerous field studies of nearshore marine units. Table 1 summarizes units described in the literature that contain paleoflow indicators and were deposited in the western half of the seaway during the Cretaceous, when the seaway was through-going.

The majority record southerly directed paleoflows. Where the indicators are cross-strata of dunes, it seems reasonable that the net sediment transport direction also was southerly. Quite remarkably, all depositional environments sampled, whether the foreshore, shoreface, shelf, or incised estuarine valleys, show this southerly transport. Even estuarine valley-fills cut at low-stand—such as suggested for the Shannon, the Tocito, the Sego sandstones—all contain south-directed paleoflow indicators. Why rivers feeding a roughly north-south shoreline should have turned south, paralleling the shore as they extended seaward during low-stand remains a puzzle. Jennette et al. (1995) call upon tectonic control, but the evidence is circumstantial. Here we propose that the rivers inherited a shelf bathymetry of southerly recurved, subaqueous spits and shoals created by deflection of delta plumes at highstand. Therefore, as sea level fell, the rivers were steered south to debouch on local east-west trending shorelines.

CONCLUSIONS

Our modeling results indicate that net sediment transport along the western margin of the seaway—whether in offshore sand ridges, incised estuarine valley fills, or incised shoreface deposits—would have been to the south. This occurred because the mean annual wind field, latitudinal temperature gradient, and fresh water runoff from land created a background circulation consisting of southerly geostrophic flow on the western shelf. In addition, counterclockwise-rotating, mid-latitude cyclonic storms passing southeastward over the central seaway drive a net southerly littoral drift in the foreshore and shore-parallel geostrophic flows whose net suspended load transport is southerly. Finally, one can conjecture that in response to these mean and event-generated southerly flows, sediment plumes at river mouths constructed submarine topographies at highstand that recurved southward. When sea level fell, river courses may have been steered by this subtle topography to incise shore-parallel or oblique valleys filled with southerly directed, estuarine valley-fill sandbodies

←

Fig. 5.—Dark patches denote regions of significant wave-current shear velocities ($U_{*cw} > 1$ cm/s) computed from the benthic boundary layer model. (a) High shear velocities occur along the western margin as the storm enters the seaway. (b) High shear velocities occur on both the western and eastern shelves as the storm crosses midway. (c) High shear velocities are limited to the eastern margin. Maximum shear velocities remained at about 8 cm/s throughout the storm's passage but changed location. For reference, bed shear stress is proportional to U^2_{*cw}.

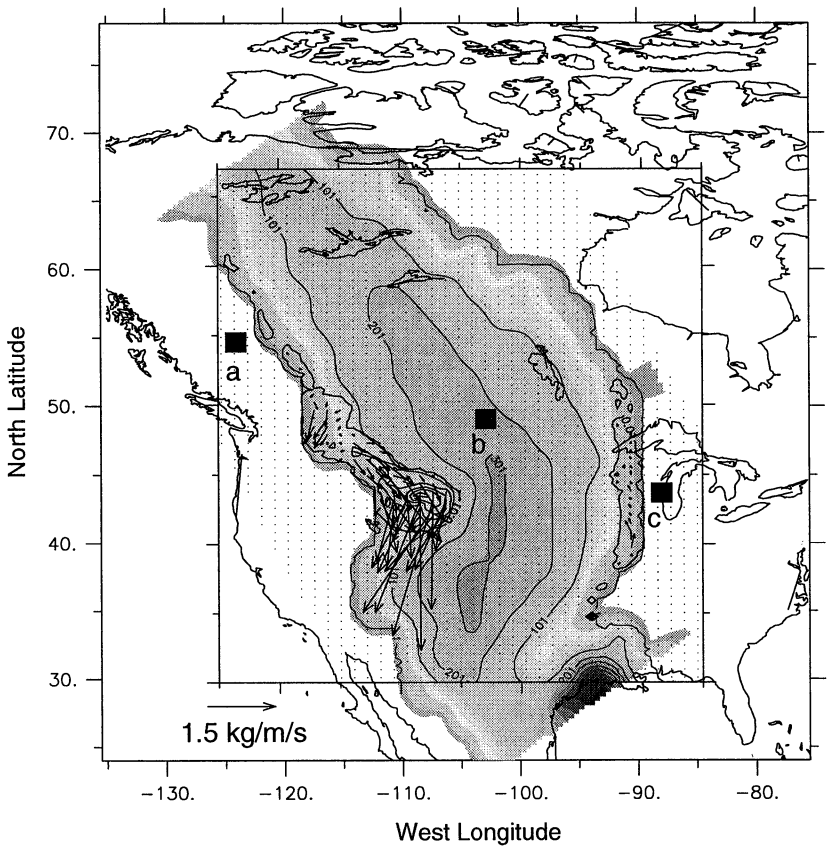

Fig. 6.—Net direction and magnitude of transport of suspended load (kg/m/s) during the eight days of the storm. Values reflect integration of sediment concentration over the lower 10 m of the water column times wind-driven current speed in lowest layer of POM expressed as kg per unit width per unit time.

ACKNOWLEDGMENTS

R. Slingerland was supported in part by National Science Foundation grant EAR-9117398; T. R. Keen was supported by Program Element 62435N of the Office of Naval Research. We thank J. T. Parrish and D. A. Leckie for their comments on the manuscript,

REFERENCES

BARRON, E.J., 1987, Cretaceous paleogeography: Palaeogeography, Palaeoclimatology, Palaeoecology, v. 40, p. 103-133.

BARRON, E.J., FAWCETT, P.J., POLLARD, D. AND THOMPSON, S.L., 1993, Model simulations of Cretaceous climates: The rope of geography and carbon dioxide: Philosophical Transactions of the Royal Society of London B, v. 341, p. 307-316.

BERGMAN, K.M., 1994, Shannon Sandstone in Hartzog Draw-Heldt Draw fields (Cretaceous, Wyoming, USA) reinterpreted as lowstand shoreface deposits, Journal of Sedimentary Research, Section B: Stratigraphy and Global Studies, v. 64, p. 184-201.

BHATTACHARYA, J., WALKER, R.G., 1991, River- and wave-dominated depositional systems of the Upper Cretaceous Dunvegan Formation, northwestern Alberta, Bulletin of Canadian Petroleum Geology, v. 39, p. 165-191.

BLUMBERG, A.F. AND MELLOR, G.L., 1987, A description of a three-dimensional coastal ocean circulation model, *in* Heaps, N.S., ed., Three Dimensional Coastal Ocean Models: Washington, D.C., American Geophysical Union Coastal and Estuarine Sciences Series, v. 4, p. 1-16.

BOYLES, J.M. AND SCOTT, A.J., 1982, A model for migrating shelf bar sandstones in Upper Mancos Shale (Campanian), northwestern Colorado: American Association of Petroleum Geologists Bulletin, v. 66, p. 491-508.

CAMPBELL, C.V., 1971, Depositional model Upper Cretaceous Gallup beach shoreline, Ship Rock area, northwestern New Mexico: Journal of Sedimentary Petrology, v. 41, p. 395-409.

CORPS OF ENGINEERS, 1984, Shore Protection Manual, 4th ed. Vicksburg, Miss., Dept. of the Army, Waterways Experiment Station, Coastal Engineering Research Center, Washington, D.C.

COTTER, E., 1975, Late Cretaceous sedimentation in a low-energy coastal zone: The Ferron Sandstone of Utah: Journal of Sedimentary Petrology, v. 45, p. 669-685.

DOWNING, K.P., WALKER, R.G., 1988, Viking Formation, Joffre Field, Alberta; shoreface origin of long, narrow sand body encased in marine mudstones: American Association of Petroleum Geologists Bulletin, v. 72, p. 1212-1228.

ERICKSEN, M.C. AND SLINGERLAND, R., 1990, Numerical simulations of tidal and wind-driven circulation in the Cretaceous Interior seaway of North America: Geological Society of America Bulletin, v. 102, p. 1499-1516.

EVANS, W.E., 1970, Imbricate linear sandstone bodies of Viking Formation in Dodsland-Hoosier area of southwestern Saskatchewan, Canada: The American Association of Petroleum Geologists Bulletin, v. 54, p. 469-486.

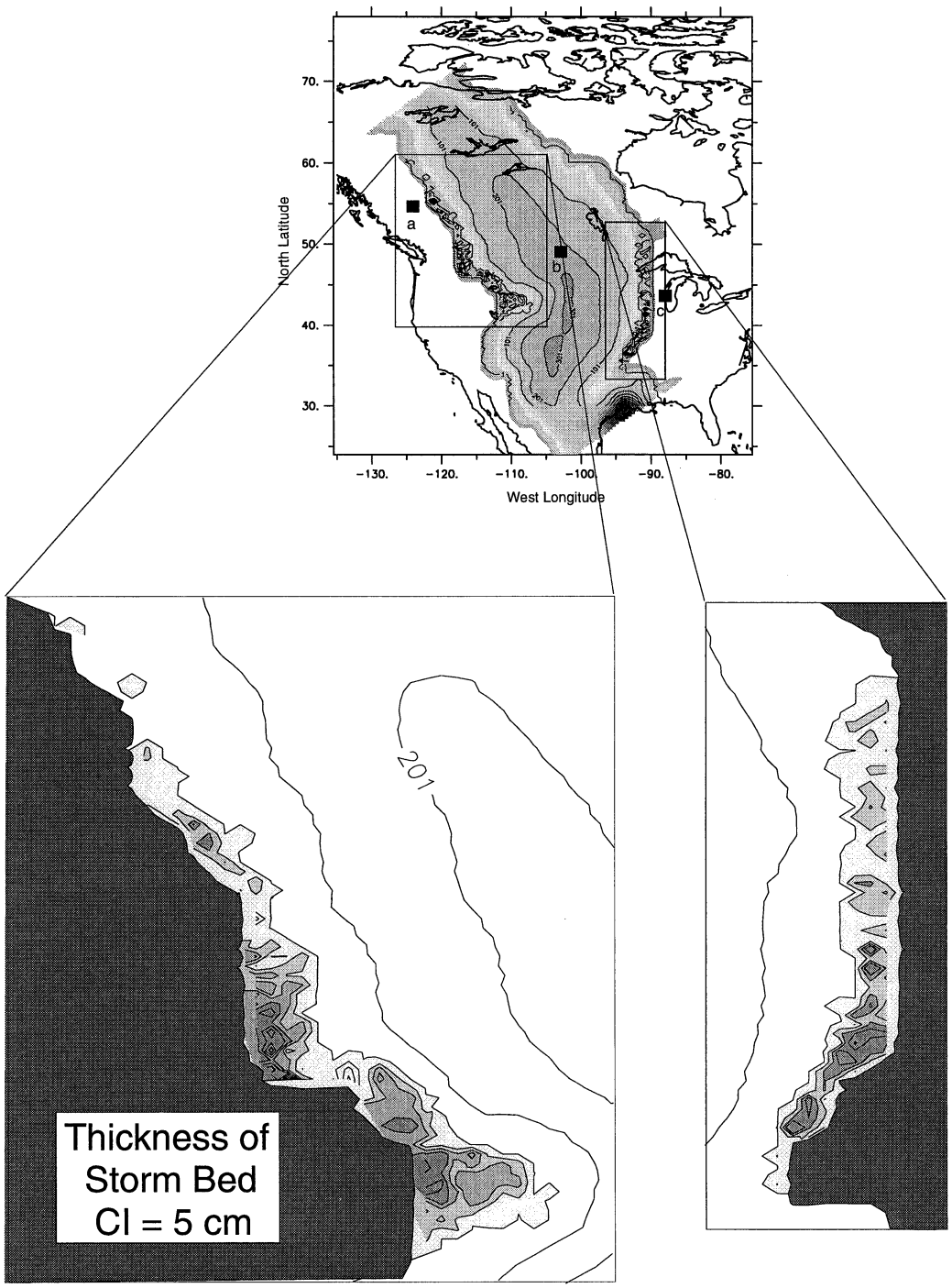

Fig. 7.—Thickness (cm) of storm bed deposited during the 8-day simulation. Lightest shading denotes region of bed thickness between 0 and 5 cm. A bed extends to depths of 75 m along the western margin where flow was strongest. The bed is limited to depths of about 20 m along the eastern margin.

FITZSIMMONS, R.O., 1995, High resolution sequence stratigraphy of the Upper Cretaceous Eagle Formation, Wyoming, U.S.A., *in* Fitzsimmons, R.O., Parsons, B. and Swift, D.J.P., eds., Tongues, Ridges, and Wedges, Society of Economic Paleontologists and Mineralogists Research Conference Field Guide, June 24-29, 1995, p. 29.

GAYNOR, G.C., SWIFT, D.J.P., 1988, Shannon Sandstone depositional model; sand ridge dynamics on the Campanian Western Interior Shelf, Journal of Sedimentary Petrology, v. 58, p. 868-880.

GLENN, S.M. AND GRANT, W.D., 1987, A suspended sediment stratification correction for combined wave and current flows: Journal Geophysical Research, v. 92, p. 8244-8264.

Table 1.—Paleocurrent data from nearshore marine sandbodies along the western margin of the Cretaceous Western Interior seaway.

Unit	Age	Depositional Environments and Paleocurrent Data
1. Tocito Ss.; northwestern New Mexico (Van Wagoner, et al., 1991)	Coniacian	Transgressive shelf sand ridge or incised estuarine valley: offshore unimodal large-scale cross-strata dip to SE; large wave-ripple crests trend NW-SE; shore parallel sediment transport to the SE on a transgressive restricted shelf or SE transport in a shore-parallel estuary
2. Kenilworth Mbr., Blackhawk Fm.; Book Cliffs, Utah (Taylor and Lovell, 1995)	Campanian	Upper shoreface: "Trough cross-bed orientations...in the upper shoreface deposits...have a dominant southerly component and suggest that there were strong shore-parallel currents."
3. Shannon Ss., east-central Wyoming (Tillman and Martinsen, 1984)	Campanian	Shelf ridge complex: "Transport directions determined from high-angle cross-beds indicate a southwest transport direction."
4. Dunvegan Fm.; northwestern Alberta (Bhattacharya and Walker, 1991)	Cenomanian	Barrier bar: "A major distributary channel probably fed this barrier bar at its northeastern end and sand was transported to the southwest by longshore drift."
5. Burnstick Mbr., Cardium Fm.; Alberta (Pattison and Walker, 1992)	Turonian	Incised shoreface: "We interpret the alongstrike trends as the result of ... southwestward sediment transport in the shoreface."
6. Virgelle Mbr, Eagle Fm.; Bighorn Basin, Wyoming (Fitzsimmons, 1995)	Campanian	Incised estuarine valley: bipolar N-S dipping trough cross-strata fill a N-S trending, shore parallel, incised valley
7. Baytree Mbr., Cardium Fm.; northwestern Alberta (Hart and Plint, 1989)	Turonian	Shoreface: "The dominant southeast (i.e. shore-parallel) cross-bedding, in both sandstones and conglomerates indicates a strong longshore component to sediment transport."
8. Rusty Mbr., Ericson Ss.; SW Wyoming (Martinsen et al., 1997)	Campanian	Valley-fill sandstones: "In contrast to surrounding delta plain sediments, where paleoflow was to the ESE, the paleocurrents within valley-fill sandstones are directed to the SSW."
9. Duffy Mtn. Ss., Mancos Shale; Northwestern Colorado (Boyles and Scott, 1982)	Campanian	Shore-parallel shelf bars: " The sediment was probably derived from....southwestern Wyoming."
10. Eagle Ss.; north-central Montana (Rice, 1980)	Upper Cretaceous	Delta-front: "The sand was probably deposited as river-mouth bars that were redistributed by dominately southward-flowing marine longshore currents..."
11. Gallop Ss.; northwestern New Mexico (Campbell, 1971)	Upper Cretaceous	Elongate, shore-parallel, northwest-southeast trending, offshore bar: Cross-laminae dip to the southeast.
12. Ferron Ss.; Castle Valley, Utah (Cotter, 1975)	Upper Cretaceous	Low energy coast: "Sediment....was derived from the large Vernal Delta, located north and west of the Castle Valley outcrops, and was transported generally southwestward, parallel with the coast."
13. Hygiene Ss.; northern Colorado (Kitely and Field, 1984)	Late Campanian	Mid-outer shelf sand ridges: "The sand was derived from the west, transported eastward, and then redistributed by southward-flowing storm and oceanic currents."

GRANT, W.D. AND MADSEN, O.S., 1982, Movable boundary roughness in unsteady oscillatory flow: Journal Geophysical Research, v. 87, p. 1797-1808.

GREEN, M.O., VINCENT, C.E., MCCAVE, I.N., DICKSON, R.R., REES, J.M. AND PEARSON, N.D., 1995, Storm sediment transport; observations from the British North Sea shelf: Continental Shelf Research, v. 15, p. 889-912.

HART, B.S., PLINT, A.G., 1989, Gravelly shoreface deposits; a comparison of modern and ancient facies sequences: Sedimentology, v. 36, p. 551-557.

HAY, W.W., EICHER, D.L. AND DINER, R., 1993, Physical oceanography and water masses in the Cretaceous Western Interior seaway, *in* Caldwell, W.G.E. and Kauffman, E.G., eds., Evolution of the Western Interior Basin: St. John's, Geological Association of Canada Special Paper 39, p. 297-318.

HEIN, F.J., DEAN, M.E., DEIURE, A.M., GRANT, S.K., ROBB, G.A., LONGSTAFFE, F.J., 1986, The Viking Formation in the Caroline, Garrington and Harmattan East fields, western south-central Alberta; sedimentology and paleogeography: Bulletin of Canadian Petroleum Geology, v. 34, p. 91-110.

JENNETTE, D.C., JONES, C.R., 1995, Sequence stratigraphy of the Upper Cretaceous Tocito Sandstone; a model for tidally influenced incised valleys, San Juan Basin, New Mexico, *in* Van Wagoner, J.C., Bertram, G.T., Sequence stratigraphy of foreland basin deposits; outcrop and subsurface examples from the Cretaceous of North America: American Association of Petroleum Geology Memoir, v. 64, p. 311-347.

JEWELL, P.W., 1996, Circulation, salinity, and dissolved oxygen in the Cretaceous North American seaway: American Journal of Science, v. 296, p. 1093-1125.

KEEN, T.R. AND GLENN, S.M., 1994, A coupled hydrodynamic-bottom boundary layer model of Ekman flow on stratified continental shelves: Journal of Physical Oceanography, v. 24, p. 1732-1749.

KEEN, T.R. AND SLINGERLAND, R.L., 1993, A numerical study of sediment transport and event bed genesis during Tropical Storm Delia: Journal of Geophysical Research, v. 98, p. 4775-4791.

KITELEY, L.W., FIELD, M.E., 1984, Shallow marine depositional environments in the Upper Cretaceous of northern Colorado, *in* Tillman, R.W. and Siemers, C.T., Siliciclastic shelf sediments: Tulsa, Society of Economic Paleontologists and Mineralogists Special Publication, 34, p. 179-204.

LECKIE, D.A., 1986, Tidally influenced, transgressive shelf sediments in the Viking Formation, Caroline, Alberta: Bulletin of Canadian Petroleum Geology, v. 34, p. 111-125.

LEE, T.N., KOURAFALOU, V., WNAG, J.D. AND HO, W.J., 1985, Shelf circulation from Cape Canaveral to Cape Fear during Winter; *in* Atkinson, L.P., Menzel, D.W. and Bush, K.A., Oceanography of the Southeastern U.S. Continental Shelf: Washington, D.C., American Geophysical Union Coastal and Estuarine Sciences, v. 2, p. 33-62.

LEENDERTSE, L.J. AND LIU, S.K., 1977, A three-dimensional model for estuaries and coastal seas: v. IV, turbulent energy computation: Santa Monica, Rand Report Number R-2187-OWRT.

MADSEN, O.S., WRIGHT, L.D., BOON, J.D. AND CHISHOLM, T.A., 1993, Wind stress, bed roughness and sediment suspension on the inner shelf during an extreme storm event, *in* Huntley, D.A., Nearshore and coastal oceanography: Continental Shelf Research, v. 13, p. 1303-1324.

MARTINSEN, O.J., RYSETH, A. AND HELLAND-HANSEN, W., 1997, Sandrich, estuarine valley-fill sandstones, Rust Member, Ericson Sandstone (Campanian), SW Wyoming: Sedimentology, stratigraphy, and tectonic significance (abs.): Society of Economic Paleontologists and Mineralogists—Canadian Society of Petroleum Geologists Joint Convention, p. 184.

MELLOR, G.L., 1993, Users Guide for a Three-dimensional, Primitive Equation, Numerical Ocean Model. Report to the Institute of Naval Oceanography: Princeton, New Jersey, Princeton University, 35 p.

MELLOR, G.L. AND YAMADA, T., 1982, Development of a turbulence closure model for geophysical fluid problems: Review of Geophysics and Space Physics, v. 20, p. 851-875.

NUMMEDAL, D. AND RILEY, G.W., 1991, Origin of late Turonian and Coniacian unconformities in the San Juan Basin, *in* Van Wagoner, J.C., Jones, C.R., Taylor, D.R., Nummedal, D., Jennette, D.C. and Riley, G.W., Sequence stratigraphy applications to shelf sandstone reservoirs; outcrop to subsurface examples: American Association of Petroleum Geologists Field Conference, p. 1-6.

PARRISH, J.T., GAYNOR, G.C. AND SWIFT, D.J.P., 1984, Circulation in the Cretaceous Western Interior seaway of North America, a review, *in* Stott, D.F. and Glass, D.J., (eds), The Mesozoic of Middle North America: Canadian Society of Petroleum Geologists Memoir, v. 9, p. 221-231.

PATTISON, S.A.J., WALKER, R.G., 1992, Deposition and interpretation of long, narrow sandbodies underlain by a basinwide erosion surface; Cardium Formation, Cretaceous Western Interior seaway, Alberta, Canada: Journal of Sedimentary Petrology, v. 62, p. 292-309.

POLLARD, D. AND THOMPSON, S.L., 1992, User's Guide to the GENESIS Global Climate Model Version 1.02: Boulder, National Center for Atmospheric Research ICS, 58 p.

POSAMENTIER, H.W. AND CHAMBERLAIN, C.J., 1993, Sequence-stratigraphic analysis of Viking Formation lowstand beach deposits at Joarcam Field, Alberta, Canada, *in* Posamentier, H.W., Summerhayes, C.P., Haq, B.U. and Allen, G.P., Sequence stratigraphy and facies associations: International Association of Sedimentologists Special Publication, 18, p. 469-485.

POWER, B.A., 1988, Coarsening-upwards shoreface and shelf sequences; examples from the Lower Cretaceous Viking Formation at Joarcam, Alberta, Canada, *in* James, D.P. and Leckie, D.A., Sequences, stratigraphy, sedimentology; surface and subsurface: Canadian Society of Petroleum Geologists Memoir, v. 15, p. 185-194.

RADDYSH, H.K., 1988, Sedimentology and "geometry" of the Lower Cretaceous Viking Formation, Gilby A and B fields, Alberta, *in* James, D.P. and Leckie, D.A., Sequences, stratigraphy, sedimentology; surface and subsurface: Canadian Society of Petroleum Geologists Memoir, v. 15, p. 417-429.

RICE, D.D., 1976, Depositional environments of Eagle Sandstone, North-central Montana; aid for hydrocarbon exploration, American Association of Petroleum Geologists Bulletin, v. 60, p. 1408.

RICE, D.D., 1980, Coastal and deltaic sedimentation of Upper Cretaceous Eagle Sandstone; relation to shallow gas accumulations, North-central Montana: American Association of Petroleum Geologists Bulletin, v. 64, p. 316-338.

RICE, D.D., SHURR, G.W., 1983, Patterns of sedimentation and paleogeography across the Western Interior seaway during time of deposition of Upper Cretaceous Eagle Sandstone and equivalent rocks, Northern Great Plains, *in* Reynolds, M.W., Dolly, E.D., Mesozoic paleogeography of the West-Central United States: Rocky Mountain Paleogeography Symposium, v. 2, p. 337-358.

SAGEMAN, B.B. AND ARTHUR, M.A., 1994, Early Turonian paleogeographic/paleobathymetric map, Western Interior, US, *in* Caputo, M.V., Peterson, A. and Franczyk, K.J., eds., Mesozoic Systems of the Rocky Mountain Region, USA: Tulsa, Society of Economic Paleontologists and Mineralogists, Rocky Mountain Section, p. 457-469.

SEELING, A., 1978, The Shannon Sandstone, a further look at the environment of deposition at Heldt Draw Field, Wyoming, The Mountain Geologist, v. 15, p. 133-144.

SHURR, G.W., 1984, Geometry of shelf-sandstone bodies in the Shannon Sandstone of southeastern Montana, *in* Tillman, R.W. and Siemers, C.T., Siliciclastic shelf sediments: Tulsa, Society of Economic Paleontologists and Mineralogists Special Publication, 34, p. 63-83.

SLATER, R.D., 1985, A numerical model of tides in the Cretaceous seaway of North America: Journal of Geology, v. 93, p. 333-345.

SLINGERLAND, R., KUMP, L.R., ARTHUR, M.A., FAWCETT, P.J., SAGEMAN, B.B. AND BARRON, E.J., 1996, Estuarine circulation in the Turonian-Western Interior seaway of North America: Geological Society of America Bulletin, v. 108, p. 941-952.

SNEDDEN, J.W. AND NUMMEDAL, D., 1990, Coherence of surf zone and shelf current flow on the Texas (U.S.A.) coastal margin; implications for interpretation of paleo-current measurements in ancient coastal sequences: Sedimentary Geology, v. 67, p. 221-236.

SPEARING, D.R., 1976, Upper Cretaceous Shannon Sandstone; an offshore, shallow-marine sand body: Casper, Wyoming Geological Association Guidebook, v. 28, p. 65-72.

SWIFT, D.J.P., YOUNG, R.A., CLARKE, T.L., VINCENT, C.E., NIEDORODA, A. AND LESHT, B., 1979, Sediment transport in the Middle Atlantic Bight of North America; synopsis of recent observations, *in* Nio, S.D., Shuettenhelm, R.T.E., van Weering, T.C.E., Holocene marine sedimentation in the North Sea basin: International Association of Sedimentologists Special Publication, v. 5, p. 361-383.

SWIFT, D.J.P., RICE, D.D., 1984, Sand bodies on muddy shelves; a model for sedimentation in the Western Interior seaway, North America, *in* Tillman, R.W. and Siemers, C.T., Siliciclastic shelf sediments: Tulsa, Society of Economic Paleontologists and Mineralogists Special Publication, 34, p. 43-62.

TAYLOR, D.R. AND LOVELL, R.W.W., 1995, High-frequency sequence stratigraphy and paleogeography of the Kenilworth Member, Blackhawk Formation, Book Cliffs, Utah, U.S.A., *in* Van Wagoner, J.C. and Bertram, G.T., Sequence stratigraphy of foreland basin deposits; outcrop and subsurface examples from the Cretaceous of North America: American Association of Petroleum Geologists Memoir, v. 64, p. 257-275.

TILLMAN, R.W. AND MARTINSEN, R.S., 1984, The Shannon shelf-ridge sandstone complex, Salt Creek Anticline area, Powder River basin, Wyoming, *in* Tillman, R.W., Siemers, C.T., Siliciclastic shelf sediments: Tulsa, Society of Economic Paleontologists and Mineralogists Special Publication, 34, p. 85- 142.

TILLMAN, R.W., MARTINSEN, R.S., 1987, Sedimentologic model and production characteristics of Hartzog Draw Field, Wyoming, a Shannon shelf-ridge sandstone, *in* Tillman, R.W. and Weber, K.J., Reservoir sedimentology: Tulsa, Society of Economic Paleontologists and Mineralogists Special Publication, 40, p. 15-112

VALASEK, D., 1995, The Tocito Sandstone in a sequence stratigraphic framework; an example of landward- stepping small-scale genetic sequences, *in* Van Wagoner, J.C. and Bertram, G.T., Sequence stratigraphy of foreland basin deposits; outcrop and subsurface examples from the Cretaceous of North America: American Association of Petroleum Geologists Memoir, v. 64, p. 349-369.

VAN WAGONER, J.C., JONES, C.R., TAYLOR, D.R., NUMMEDAL, D., JENNETTE, D.C. AND RILEY, G.W., 1991, Sequence stratigraphy applications to shelf sandstone reservoirs; outcrop to subsurface examples: Tulsa, American Association of Petroleum Geologists Field Conference Guidebook.

VINCENT, C.E., YOUNG, R.A. AND SWIFT, D.J.P., 1983, Sediment transport on the of Long Island shoreface, North American Atlantic shelf; role of wave and currents in shoreface maintenance: Continental Shelf Research, v. 2, p. 163-181.

WALKER, R.G., 1995, Sedimentary and tectonic origin of a transgressive surface of erosion; Viking Formation, Alberta, Canada: Journal of Sedimentary Research, Section B: Stratigraphy and Global Studies, v. 65, p. 209-221.

WALKER, R.G. AND WISEMAN, T.R., 1995, Lowstand shorefaces, transgressive incised shorefaces, and forced regressions; examples from the Viking Formation, Joarcam area, Alberta: Journal of Sedimentary Research, Section B: Stratigraphy and Global Studies, v. 65, p. 132-141.

WALKER, R.G. AND BERGMAN, K.M., 1993, Shannon Sandstone in Wyoming; a shelf-ridge complex reinterpreted as lowstand shoreface deposits: Journal of Sedimentary Petrology, v. 63, p. 839-851.

WRIGHT, L.D., XU, J.P. AND MADSEN, O.S., 1994, Across-shelf benthic transports on the inner shelf of the Middle Atlantic Bight during the "Halloween storm" of 1991: Marine Geology, v. 118, p. 61-77.